HAL
archives-ouvertes.fr

Detailed β-decay study of 32Ar

R. Dominguez-Reyes, N. Adimi, M. Alcorta, A. Bey, M.J.G. Borge, M. Carmona-Gallardo, F. de Oliveira Santos, C. Dossat, H.O.U. Fynbo, J. Giovinazzo, et al.

▶ **To cite this version:**

R. Dominguez-Reyes, N. Adimi, M. Alcorta, A. Bey, M.J.G. Borge, et al.. Detailed β-decay study of 32Ar. 2011. in2p3-00617510

HAL Id: in2p3-00617510
http://hal.in2p3.fr/in2p3-00617510

Preprint submitted on 29 Aug 2011

HAL is a multi-disciplinary open access archive for the deposit and dissemination of scientific research documents, whether they are published or not. The documents may come from teaching and research institutions in France or abroad, or from public or private research centers.

L'archive ouverte pluridisciplinaire **HAL**, est destinée au dépôt et à la diffusion de documents scientifiques de niveau recherche, publiés ou non, émanant des établissements d'enseignement et de recherche français ou étrangers, des laboratoires publics ou privés.

Detailed β-decay study of ^{32}Ar

R. Domínguez-Reyes[1], N. Adimi[2,3], M. Alcorta[1], A. Bey[2], B. Blank[2], M.J.G. Borge[1], M. Carmona-Gallardo[1], F. de Oliveira Santos[4], C. Dossat[2], H.O.U. Fynbo[5], J. Giovinazzo[2], H.H. Knudsen[5], M. Madurga[1], I. Matea[2,6], A. Perea[1], K. Sümmerer[7], O. Tengblad[1], and J.C. Thomas[4]

[1] Instituto de Estructura de la Materia, IEM-CSIC, C/Serrano 113bis, E-28006, Madrid, Spain.
[2] Centre d'Études Nucléaires de Bordeaux Gradignan, Université Bordeaux 1, UMR 5797 CNRS/IN2P3, Chemin du Solarium, BP 120, F-33175 Gradignan, France.
[3] Faculté de Physique, USTHB, B.P.32, El Alia, 16111 Bab Ezzouar, Alger, Algeria.
[4] Grand Accélérateur National d'Ions Lourds, CEA/DSM-CNRS/IN2P3, B.P. 55027, F-14076 Caen Cedex 05, France
[5] Department of Physics and Astronomy, University of Aarhus, Ny Munkegade 1520, DK-8000 Aarhus C, Denmark
[6] Institut de Physique Nucléaire, CNRS-IN2P3 / Université Paris-Sud 11, Orsay, France
[7] GSI Helmholtzzentrum für Schwerionenforschung GmbH, Planckstrasse 1, D-64291 Darmstadt, Germany

E-mail: mj.borge@csic.es

Abstract. Beta-delayed proton and γ-ray emission from the ^{32}Ar decay has been studied at the low-energy identification station of SPIRAL at GANIL. The study of β-delayed charged-particle emission and electromagnetic radiation allowed us to achieve a nearly complete decay scheme of the ^{32}Ar nucleus. With the distinction between β-delayed protons emitted to the ground and to the first excited state in ^{31}S and the new values of half-life and Q_{EC} we have deduced the Gamow-Teller strength distribution over a large part of the Q_{EC} window. The GT strength is compared to advanced shell-model calculations. The experimental Gamow-Teller strength is wider distributed than theoretically predicted and the onset of the Gamow-Teller Giant Resonance happens at lower energy. This explains why the deduced value for the quenching factor depends strongly on the explored excitation energy in the daughter nucleus. When the energy window is chosen large enough the standard quenching factor for the sd-shell is recovered.

PACS numbers: 23.40.-s,23.50.+z,27.30.+t,29.30.Ep

Submitted to: *J. Phys. G: Nucl. Phys.*

1. Introduction

One of the most important methods to study the atomic nucleus is nuclear β decay. The very restrictive selection rules of the β-decay process make it a powerful tool to deduce information about nuclear structure. Studies close to the valley of beta stability allow us to precisely test our understanding of the structure at low excitation energies. However, in the region near the proton drip-line the differences in the isobaric masses result in a wide decay window, which extends nuclear structure studies using beta-decay towards much higher excitation energies. Due to the very low binding energy of the last proton in very proton-rich nuclei, excitation energies in the daughter nucleus beyond the proton separation energy can be explored through β-delayed particle emission.

The high sensitivity for charged-particle detection compared to γ-ray detection explains why most of the studies of light neutron-deficient nuclei have been based on charged-particle detection and the β-decay scheme was often built with the assumption that most of the β-delayed protons feed the ground state of the proton-daughter nucleus. A step further is the detection of both types of emissions providing us with a more complete scenario for nuclear-structure studies. Thanks to the fact that in nuclei with Z>N the isobaric analog state (IAS) is within the Q_{EC} window, a major part of the allowed β-decay strength can be directly measured. In the decay of ^{32}Ar, where the IAS is located in the lower half of the Q_{EC} window, we expect to detect a substantial part of the Gamow-Teller (GT) Giant Resonance (GR), or at least the onset of the GTGR. Therefore it is worth to perform a complete study with good γp information to determine the GT strength distribution and to determine the quenching factor of the Gamow-Teller strength B(GT). This factor which relates experimental and theoretical B(GT) distributions has been calculated to be substantially lower than unity in different kinds of studies, from β decay to charge-exchange reactions, in many different nuclei. Two main explanations have been proposed to cause this quenching. On the one hand, the contribution of sub-nuclear excitations, such as the Δ resonance, that may shift the transition strength to high excitation energies. On the other hand, the limited amount of nuclear orbitals taken into account in shell-model calculations to describe the transition strength. In particular, intruder orbitals giving rise to higher-energy excitations are usually not included in order to keep the model calculation tractable. Recently, the ^{90}Zr(p,n) and (n,p) reactions were measured up to 70 MeV to study the contribution to the GT strength of the continuum beyond the GTGR [1]. It was found that most of the quenching disappeared when the continuum was taken into account. It was concluded that second-order configuration mixing was the main mechanism responsible for the quenching of the Gamow-Teller strength. For details in the same direction see also the discussion in [2].

The decay of ^{32}Ar (T_z=-2) was studied several times [3, 4, 5, 6] with different aims and methods. In the first work, Hagberg *et al.* [3] managed to identify the most intense βp branch from the IAS and confirmed that the quadratic form of the isobaric multiplet mass equation (IMME) was valid also for nuclei with isospin T=2 as this was the first

isobaric quintet studied. Later, Björnstad *et al.* [4] did the first overall study of the decay properties and states in ^{32}Cl. Comparison of the B(GT) strength of the light $^{32-34}$Ar isotopes with shell model calculations indicated an almost inexistent quenching of the B(GT) strength in the energy window studied [7]. Schardt & Riisager [5] used a very small cooled detector, with very good energy resolution (8 keV FWHM), to study the proton line shapes and thus tentatively assign the transitions to the first excited state of ^{31}S through the difference in width of the proton lines in the spectrum.

The more recent work of Bhattacharya *et al.* [6] studied the superallowed 0^+ to 0^+ Fermi decay to deduce the isospin symmetry breaking corrections. To this aim the absolute branching ratio to the IAS was determined with high precision to be equal to 22.71(15)% including a 1.92(9)% γ-emission branch. This result, combined with very precise determinations of the half-life $T_{1/2}$= 100.5(3) ms and of the Q_{EC} value of the IAS obtained from mass measurements [8], allowed them to determine the IAS decay strength and from that the ft value. Comparison with the average value of the corrected $\mathcal{F}$t from T=1 superallowed transitions enabled the authors to extract an isospin mixing of the IAS of 2.1(8)%, in good agreement with a shell model prediction by Brown, ref. 3 in [6], of 2.0(4)%. This good agreement indicates the degree of reliability of shell model calculations to describe these nuclei and to deduce the quenching factor from the comparison of the experimental B(GT) distribution with the one obtained from shell-model calculations [9]. The determination of the decay of the IAS in ^{32}Cl [6] by proton and γ emission yields a more precise proton separation energy (S_p), changing from S_p=1574(7) keV [10] to S_p=1581.3(6) keV. The ground state mass of ^{32}Cl has been determined recently by measuring the ^{32}S(^{3}He,t)^{32}Cl reaction with a Q3D (quadrupole-dipole-dipole-dipole) magnetic spectrograph [11]. The value obtained agrees with the one of [10], but is more precise [11]. Furthermore the mass of ^{31}S has recently been measured with the double Penning trap JYFLTRAP [12]. These measurements result in a recommended mass excess value of ΔM(^{32}Cl)= -13334.64(57) keV and S_p=1581.06(62) keV [6, 12, 11].

In this work, we present a detailed study of the B(GT) distribution of ^{32}Ar and compare it with recent shell-model calculations. In addition, we have identified a state potentially responsible for the isospin mixing of the IAS. The main advantage of the present work is the combined high efficiency for γ-ray and charged-particle detection.

2. Experiment

The ^{32}Ar beam was produced from the fragmentation of a ^{36}Ar primary beam at 95 MeV/u from the CSS1 and CSS2 cyclotrons of GANIL in the carbon target of the SPIRAL facility. The secondary beam was ionized in an *Electron Cyclotron Resonance Ion Source* (ECRIS) to obtain the $^{32}Ar^{3+}$ low-energy beam, which was directed to the SPIRAL identification station where the experimental setup was mounted. The 30 keV ^{32}Ar beam was stopped in a 0.9 μm thick aluminised mylar foil (1 cm $\times$ 2 cm) mounted on a thin metallic frame. The beam shape and the transmission to the catcher, that was

placed in the center of the setup, were controlled by beam profilers and Faraday cups. The total ^{32}Ar data correspond to 13 hours of data taking. The average intensity of the beam at the setup was at least of 100 pps. The low energy and noble gas character of the incoming beam made possible that some ^{32}Ar ions could scape from the mylar foil.

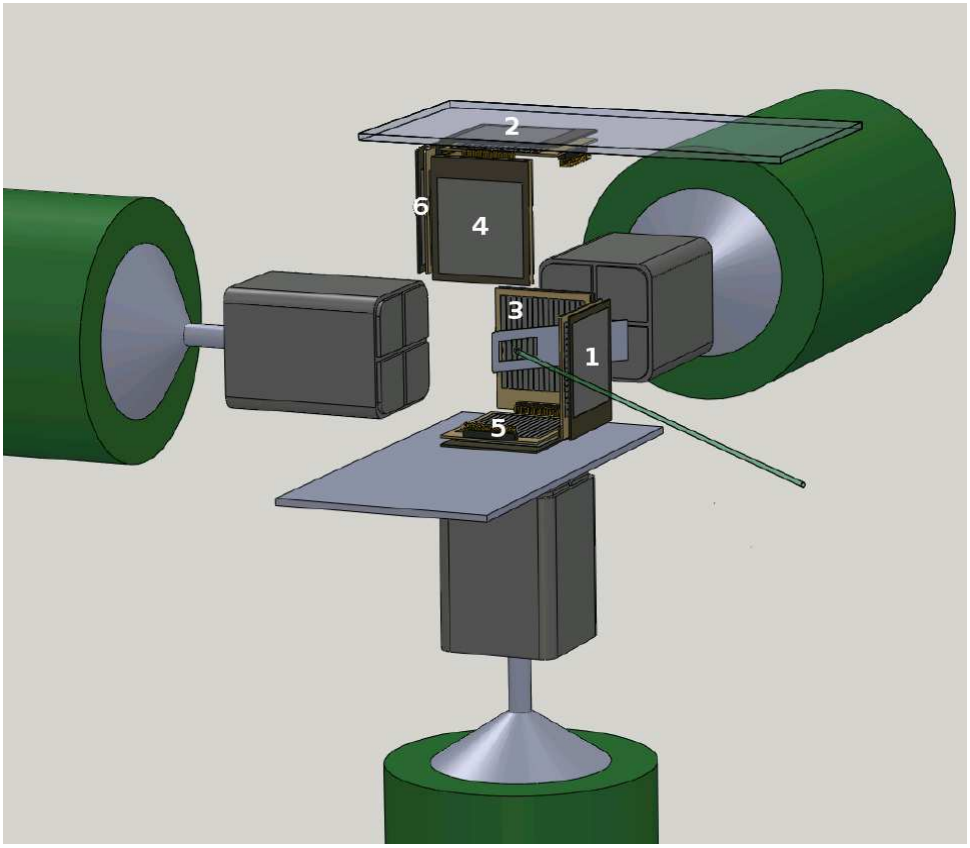

Figure 1. *Schematic drawing of the experimental setup. Three detectors of the telescope array (detectors 2, 4, and 6) have been shifted upwards in the figure to show the beam stopper (gray plate in the center of the cubic structure with a hole for the foil). The beam direction is shown by the green line.*

The setup, identical to the one used in [13], consisted of the Silicon Cube detector array [14] surrounded by three high-efficiency HPGe Clover detectors from the EXOGAM array [15]. The Silicon Cube consisted of six telescopes, formed in front by doubled-sided silicon strip detectors (DSSSDs) with 16×16 strips, and a pitch of 3 mm forming a cube facing the mylar catcher foil. These DSSSDs are backed by six large-area (50×50 mm^2) passivated implanted planar silicon (PIPS) detectors used to detect β particles. The thicknesses of the front DSSSD detectors were chosen to cover the full energy range of the decay, with 4 DSSSDs with thicknesses close to 300 μm, one thin DSSSD detector of 64 μm and one thick DSSSD of 1000 μm. The thicknesses of the back detectors of the telescopes varied from 300 to 1500 μm. The telescope on top of the catcher foil (number 2 in figure 1) did not function correctly and was not used in the present analysis. A schematic view of the detectors and the whole setup can be

seen in figure 1.

The 32×6 channels from the DSSSDs were read out via a printed circuit board incorporated in the detector housing. The 16-channel pre-amplifier cards were mounted directly onto the detector chamber allowing for a rather compact configuration. This setup had in the present experiment an effective geometrical efficiency for particle detection of 41(1)% of 4π. More details about the general performance of the Silicon Cube can be found in [14].

The three EXOGAM clover detectors surrounding the Silicon Cube consisted of 4 high-purity germanium (HPGe) crystals in a common cryostat each with a height and width of 60 mm and a length of 90 mm.

3. Calibration

We have used the spectrum of three 300 μm DSSSDs (detectors 1, 3 and 6 in figure 1) to determine the energies and intensities of the proton peaks in the region between 1.2 MeV and 5.8 MeV. For proton peaks below 1.2 MeV, the data were taken from the 64 μm detector (detector 4 in figure 1) as the β response of this detector was negligible. The region between 1.2 and 2 MeV was studied both by the 64 μm and 300 μm thick DSSSD detectors. The proton spectrum from the 1000 μm thick detector (detector 5 in figure 1) was used for proton energies above 5.8 MeV as the protons at this energy start to punch through the 300 μm thick detectors producing a decrease in the detection efficiency. Due to its thickness, this detector had a relatively large β response and worse energy resolution so its use to extract spectroscopic information was restricted to high-energy protons. To obtain the relative intensities of the proton spectra in the full energy range, the results from the 64 μm and 1000 μm thick detectors have been normalized using the relative geometric efficiency with respect to the 300 μm thick detectors and the renormalization was checked with the peak area of the IAS proton transition to the ^{31}S ground state for the 1000 μm thick detector and the 2.1 MeV proton peak in the case of the 64 μm thick detector.

The reduction of β contribution to the proton spectrum has been done in several steps. Only events which deposited energy in the front and in the back side of the DSSSD differing by less than 50 keV in the 300 and 1000 μm thick detectors were considered. In this way, effects such as charge-sharing between different strips were avoided, for more details see [16]. In order to reduce the β-summing in the 300 and 1000 μm thick detectors, the PIPS detectors were used as veto requiring the positron of the βp event to be detected in the back detector of a different telescope in order to consider a proton event valid. This led to a better resolution as well as a decrease in the β-summing and a clean low-energy part of the spectra decreasing the β contribution to the 1% level. In the case of the 64 μm thick detector, we have used its own PIPS detector as a veto for the punch-through protons in order to isolate the low energy protons that were fully stopped in the front detector.

A preliminary calibration of the charged particle detectors was performed using a

Table 1. List of γ-ray transitions in the ^{32}Ar β decay. The energies are taken from [18]. The 89.9(1) keV transition was below the detector threshold. See text for an interpretation of the γ-ray intensities given.

Nucleus	E_γ	I_γ(%) (this work)	I_γ(%) [4]
^{32}Cl	89.9(1)	-	36.5
	461.1(1)	83(17)	100
	707.4(2)	100(3)	100
	1078.7(2)	33(5)	36.5
	1168.5(2)	39(5)	37.0
^{31}S	1248.8(3)	54(6)	5.9

standard triple α-source (^{239}Pu, ^{241}Am, and ^{244}Cm). The α-source spectra allowed us to fix the noise level in the PIPS detectors in order to optimize the removal of β-summing. Due to the difference in mean energy required for a proton and α particle to create a electron-hole pair in Silicon [5, 17] it is better to use an internal calibration based on βp transitions for the DSSSDs. For the 300μm and the 1000μm detectors, we used five reference points for the internal calibration based on the most intense and most accurately determined transition energies. These transitions correspond to the proton emission from levels at excitation energies in ^{33}Cl at 3971.9(12) keV [18], 4438.2(15) keV [18], 5547.9(8) keV [19], and 6248(3) keV [18] and at 5046.3(4) keV excitation energy (IAS) in ^{32}Cl. While writing this paper a revision of the ^{33}Cl levels has been published [20], the excitation energies of the reference levels coincide within 1 keV with those used here for calibration. An additional energy correction was performed in the energy region below 1.6 MeV to account for the difference in energy losses in the stopper foil and in the detector dead layers for the low energies. For the thin 64 μm detector, as protons are only fully stopped up to 3 MeV, we used three β-delayed proton lines for the calibration. They correspond to proton transitions at 1.318, 1.643 and 2.097 MeV from the levels at 3971.9(12) keV, 4438.2(15) keV and 5868(2) keV excitation energy [18] in ^{33}Cl. The energy resolution for the proton spectrum was 70 keV for the thin detector and 45 keV (FWHM) for the thick detectors. The β-gated proton spectrum is shown in detail in figure 2. The proton spectrum is shown in two parts to facilitate the observation of details of the low intensity peaks.

The three CLOVER detectors from EXOGAM for γ detection were efficiency and energy calibrated using standard calibration sources (^{60}Co, ^{133}Ba, ^{137}Cs, ^{152}Eu and ^{207}Bi). The energy resolution (FWHM) was 6 keV at 1.3 MeV. We obtained a total efficiency of 3.0(2)% at 1249 keV, the energy of the γ ray de-exciting the first excited state in ^{31}S.

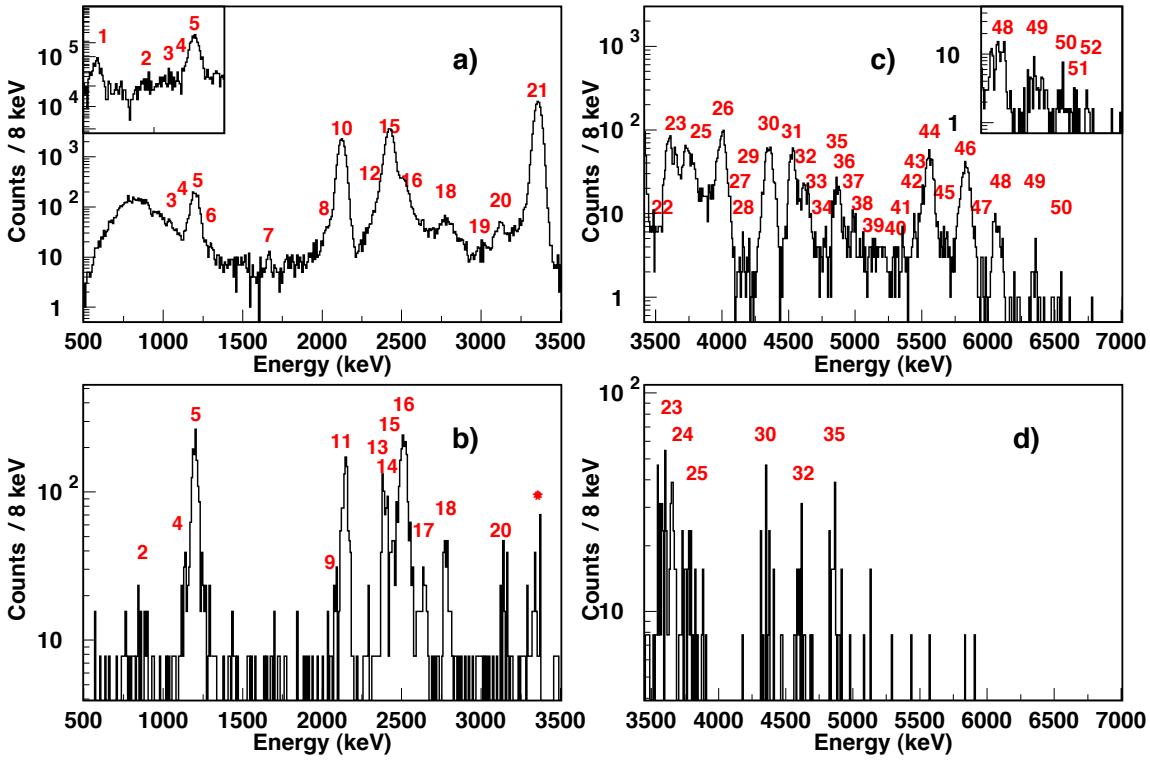

Figure 2. *(a) The β-gated proton spectrum up to 3.5 MeV from the 300 μm detectors. In the inset, the low energy part of the spectrum from the 64 μm detector is shown with a veto condition in the PIPS detector of the telescope. (b) Charged particle spectrum in coincidence with the ^{31}S 1248 keV γ-ray up to 3.5 MeV. The random coincidence level is given by the intensity of the proton peak from the IAS at 3.3 MeV marked with a star. (c) The β-gated proton spectrum above 3.5 MeV. Peaks above number 48 have been confirmed with the 1000 μm detector (inset). (d) Charged particle spectrum above 3.5 MeV in coincidence with the ^{31}S 1248 keV γ-ray.*

4. Analysis procedure

In the γ-ray spectrum, we identified (see figure 3a) γ transitions at 461.09(11), 707.4(2), 1078.5(3) and 1168.4(3) keV in ^{32}Cl (see table 1) and the 2230.3(2) keV γ transition from the ^{32}Cl decay. The 89.9(1) keV γ transition from the 89.89 keV state was below the γ threshold of some of the detectors. Throughout the experiment, the event trigger was fired only by the DSSSDs. This trigger condition strongly favours βp events over βγ events. The γ transitions in ^{32}Cl were triggered by the detection of a β particle in the DSSSDs, whereas the γ line in ^{31}S was triggered by β particles or β-delayed protons in the DSSSDs which had a much higher trigger probability. Therefore, the intensity of this last γ ray should not be compared directly to the other γ rays nor to the intensity of this line in the work of Björnstad *et al.* [4] where the trigger was different.

Despite an assignment of $J^\pi = 0^+$ or $J^\pi = 1^+$ for the 461.1 keV state in ^{32}Cl [18] we

cannot assign any β feeding to the 461.1 keV state as we get $I_\gamma(707\ \text{keV}) \geq I_\gamma(461\ \text{keV})$. Therefore, we favour a $J^\pi = 0^+$ assignment for this level as proposed by (^{3}He,t) reaction work [21, 22] and shell model predictions [23, 24]. Furthermore, no direct feeding to the states at 89.9(1) and 461.1(1) keV has previously been reported [4]. So in the following no β feeding is assumed for these states.

The data from the charged particle spectra were analyzed first assuming that all the peaks were β-delayed protons to the ground state of the daughter nucleus ^{31}S (spectra (a) and (c) in figure 2). The peaks were fitted with a Gaussian peak shape using the CERN package PAW and the centroids and the areas of the peaks were extracted.

In a second step, we analyzed the charged particle data in coincidence with γ rays. The deexcitation of the two lower excited states in ^{31}S occurs mainly by two independent γ rays of 1248.8(3) keV and 2235.5(5) keV energy, respectively. The latter could not be distinguished from the more intense 2230.3(2) keV γ-ray from the decay of ^{32}Cl. When gating on the proton spectrum the only prominent γ-ray is the 1248.8(3) keV line (see figure 3b) corresponding to the de-excitation of the first excited state of ^{31}S. Feeding from the IAS to the 2235.5(5) keV second excited state in ^{31}S of the order of 0.025(4)% is suggested in [6]. We have searched for a proton peak around 680 keV in our thin detector without success. However, a very weak indication of a relatively broad peak around 715(10) keV with a similar intensity of 0.028% was observed, but we have neglected this contribution due to the broad shape and difference with the expected energy if assumed to be a proton transition connecting the IAS to the second excited state in ^{31}S.

We selected a narrow window around the 1248.8(3) keV peak in the γ-ray spectrum to obtain the γ-gated proton spectrum and made the same selection over the background at both sides of the peak to subtract the background contributions. With this procedure, we obtained the γp coincidence spectrum that can be seen in parts (b) and (d) of figure 2. In order to determine our random coincidence level, we considered that the proton peak at 3356(2) keV comes only from the proton transition from the IAS in ^{32}Cl to the ground state of ^{31}S. The area of the γp 3356 keV peak relative to its area in the charged particle spectrum determines the random coincidence level to be 10^{-4}.

After the first analysis, it was obvious that some of the βp peaks that were assumed to correspond to transitions to the ^{31}S ground state (p_0 from now on) overlay with protons to the ^{31}S first excited state at 1248.8 keV (p_1). There are two possibilities: either some of the considered p_0 transitions in the β-gated spectrum were totally p_1 transitions, or within our energy resolution the proton peaks were found to be double with a combination of p_0 and p_1 peaks. The analysis just described was also performed for the spectra (singles and coincidence spectra) obtained with the thin detector.

To distinguish between the different possibilities, we use the fact that the γ-gated proton (γp) spectrum is clearly dominated by the proton peak at 1218(3) keV. We scaled the γp spectrum with the total γ-ray efficiency at 1248.8 keV and the extra factors due to the conditioning done to remove the β summing leading to a total normalization factor of 7.8(1). When doing this one notices that the two spectra match in intensity at

1218(3) keV as illustrated in the bottom part of figure 3. Therefore, the intensity of the 1218(3) keV proton peak can be used to scale the γp spectrum to the β-gated proton spectrum in order to obtain the p_1 branching ratios relative to those for βp decay to the ^{31}S ground state. A similar procedure to distinguish the components p_0 and p_1 from the same peak was used by Bhattacharya *et al.* [6] for the proton peak at 4527(3) keV. The contribution of β-delayed proton transitions feeding the first excited state is 5.5 % of the full proton spectrum.

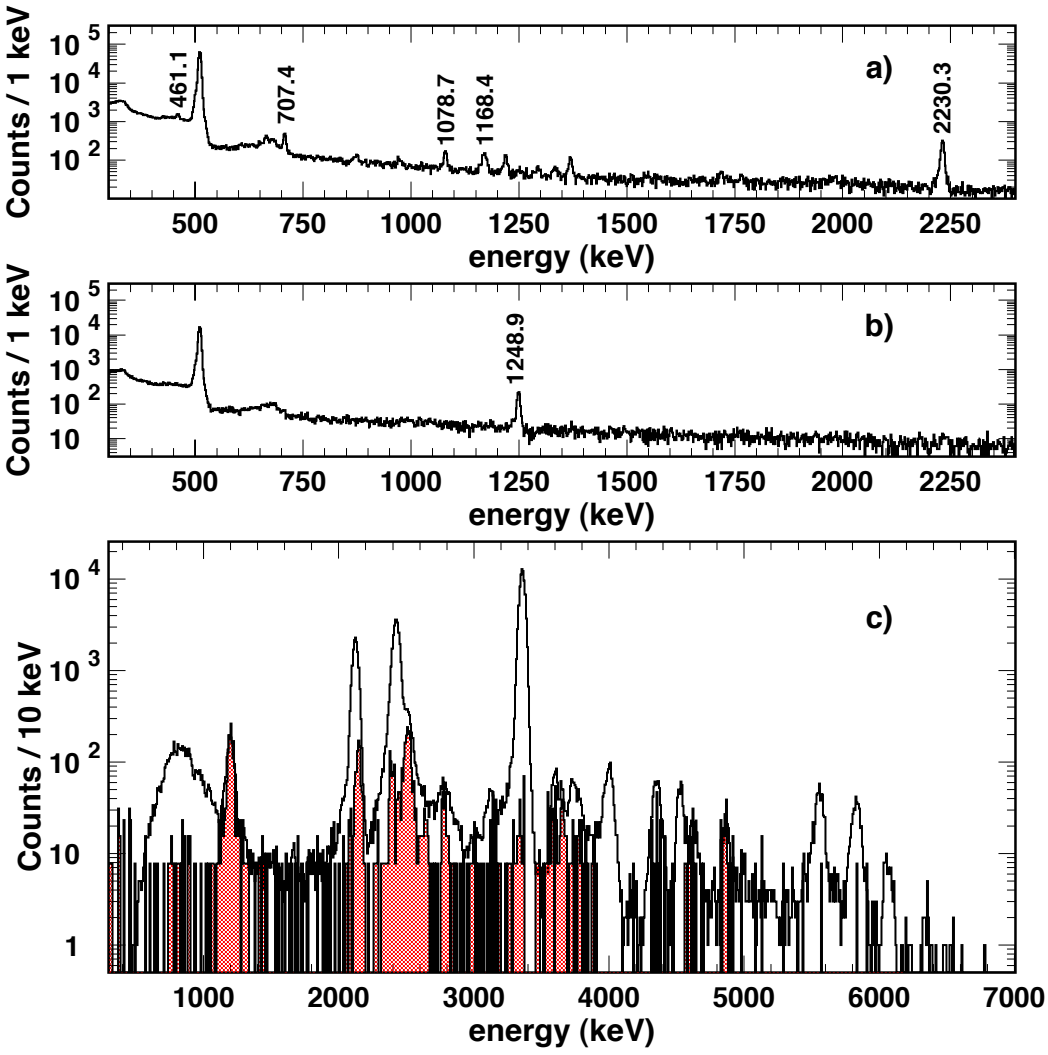

Figure 3. *a) β-gated γ-ray spectrum with the main transitions from ^{32}Ar β decay. The 2230.3(2) keV γ-ray from the decay of ^{32}Cl is also marked. b) Proton-gated γ-ray spectrum with the main transition from ^{32}Ar βp decay. Only the γ-ray from the decay of the first excited state to the ground state in ^{32}Cl is visible, whereas the γ-rays from the second excited state, expected at 986.6 keV and 2235.6 keV, are absent. c) β-gated proton spectrum (white) from the 300 μm detectors and γp spectrum (shaded) scaled to the β-gated proton spectrum with a factor 7.8(1).*

The proton peaks which have a contribution from decays to the ground and the first excited states appear with the centroid energy of the most intense contribution in table 2. They are given with their individual p_0 and p_1 centroid energies in table 3.

5. Discussion of the results

A complete list of all the proton transitions observed in this work can be found in table 2 where they are compared to the results from previous works [4, 5, 6]. For this comparison, we have corrected the βp energies determined in [4, 5] because the reference points used in their internal calibrations have changed. An internal energy calibration was performed in [4, 5] using the proton transition energies from states at 3971.9(12) and 5544(1) keV in ^{33}Cl, see compilation [18]. The latter value, from [25], was recently remeasured to be 5547.9(8) keV [19] in better agreement with the expected value from the quadratic form of the IMME formula. Due to the recently found shift of 3 keV in the IAS position of ^{33}Cl [19], we do not compare and average with previous βp energy values from [4, 5, 6], but rather state the new ones.

Comparing the excitation energies obtained from p_0 protons with energies from p_1 protons, we find many coincident values. Therefore, we could identify fourteen states that decay by proton emission both to the ground and the first excited state of ^{31}S. Only three p_1 transitions are assigned to levels with no p_0 contribution.

To determine the β feeding we calculated first the relative intensity of all proton lines with respect to the p_0 line from the IAS in ^{32}Cl (3356(2) keV proton peak) and then renormalized the results to the IAS p_0 branching ratio of 20.50(13)% recently published [6]. We have renormalized the branching ratios from [4] and the relative intensities in [5] to the new reference value, 20.50(13)%, to ease the comparison. To convert the counting rates of the γp peaks into branching ratios we used the relative intensity of the 1218(3) keV proton peak obtained in the βp spectrum.

All the proton transitions from previous studies [4, 5, 6] have been observed in this work and, due to the new γp information, we have been able to identify twice the number of proton transitions. The use of the 64 μm thick detector with a low β response enables us to identify new proton transitions below 2.1 MeV. We identified the proton peak at 603(4) keV, observed previously [4, 5, 6], but we got a much lower intensity compared to them. In order to resolve this discrepancy, we compared the ratio of the intensity of the 603 and 1218 keV proton transitions for the different strips of the thin detector and found that the ratio varies from strip to strip. We attributed this effect to the trigger thresholds for the different strips which cut the peak to some extent. As it was not possible to correct for this effect, we used for the calculation of the B(GT) distribution the average branching ratio for this proton transition from previous works [4, 5, 6]. This threshold effect did not affect the proton lines with higher energy.

The recent work of Bhattacharya *et al.* [6] gives proton transitions to the first excited state in ^{31}S and to the ground state with proton energies higher than 4 MeV plus the proton line at 610 keV. We have identified all their p_1 transitions with one

exception. In our work, we detect a prominent p_1 proton group at 2779(7) keV, not listed in [6], while they proposed a proton group at 2870(5) keV where we do not see any contribution. As they claim that the proton peak is broad, we will assume for the comparison that we are observing the same transition, although the energies differ by 90 keV. When comparing our branching ratios to those of previous works, they are in reasonable agreement in most of the cases, except for the 603 keV proton peak already mentioned and the proton lines just above the IAS where the influence of β-summing can cause the differences observed, see table 2.

Due to the enhanced γp coincidence efficiency, we have improved the quality of the measured p_1 proton spectrum. Most likely due to the low statistics of the γp spectrum in [4] where only six p_1 transitions were identified, the authors assumed that all γp transitions observed were fully feeding the ^{31}S first excited state. So the main discrepancy with previous works is the assignment of the proton peaks to the different possible transitions. For instance, the 2424(2) and 4352(3) keV peaks were assigned previously to the ^{31}S ground state only, a weak transition to the ^{31}S first excited state has been found in this work. The 2514(5) and 2779(7) keV peaks were assigned either to the ground state [4, 5] or to the excited state [6], both branches could be disentangled in our work. The proton peak at 4527(3) keV has been reported to correspond to a p_1 transition in [4], but no clear indication was found in our γp spectrum although a weak component at the level stated in [6] could not be excluded. On the contrary, a proton line at 3123 keV was assigned as a transition to the ^{31}S ground state [4]. But, this proton peak was identified in our work to feed the first excited state in ^{31}S, so the previously proposed level at 4788(20) keV [4] was moved to an excitation energy of 6066(2) keV. A level at this excitation energy was already identified both by β-decay [4] and reaction work [21]. More detailed information can be extracted by looking at table 3. This re-organization of the assignments modified the B(GT) distribution at high excitation energies.

The ^{32}Ar and ^{31}S masses have been measured using Penning traps [8, 12] and the mass of ^{32}Cl was revisited by measuring the ^{32}S(^{3}He,t)^{32}Cl reaction with a Q3D magnetic spectrograph [11]. With these values we get a Q_{EC} = 11134.4(19) keV that together with the ^{32}Ar half-life of $T_{1/2}$=100.5(3) ms [6], and the absolute branching ratios, allowed for the determination of the log(ft) values for all states.

In table 3, the excitation energies in ^{32}Cl determined from the observed protons and γ-rays are compared with the states determined by the ^{32}S(p,n) [26] and ^{32}S(^{3}He,t) [21, 27] reaction studies. The ^{32}S(p,n) reaction was measured at 135 MeV by a time-of-flight technique. This measurement gives an estimate of the ^{32}Cl resonance positions. The uncertainties given in table 3 were added by the reviewer in the compilation work [18]. We have chosen to compare with the resonant states deduced in the ^{32}S(^{3}He,t) reaction work of [21] directly because the 11 keV shift in the ^{32}Cl excitation energy added by the rewiewer seems to be valid for low energy states but not over the full excitation energy range. The advantage of populating the states by β-decay is that the feeding to 1^+ states is strongly favoured.

Table 2. List of observed β-delayed proton transitions from ^{32}Ar decay. The numbering corresponds to the labels in figure 2. Transitions to the first exited state in ^{31}S at 1248 keV are marked with #. The branching ratios are compared with values from previous works [5, 4, 6]. The values from [4, 5] were renormalized to the new value of the branching ratio for the IAS [6].

Peak Number	E_p(keV) This Work	BR (%) This Work	BR (%) Ref. [4]	BR (%) Ref. [5]	BR (%) Ref. [6]
1	603(4)	0.094(5)[a]	0.35(6)	0.42(21)	0.385(8)
2	909(10)	0.029(3)#			0.014(8)#
3	1035(10)	0.034(4)			
4	1130(10)	0.023(3)#			
5	1218(3)	0.35(3)#	0.37(4)#	0.46(10)#	0.39(4)#
6	1302(2)	0.006(1)			
7	1664(3)	0.051(2)			
8	2025(7)	0.048(2)			
9	2087(5)	0.022(5)#			
10	2123(3)	3.8(2)	3.9(4)	3.7(10)	
11	2146(3)	0.23(2)#		0.21(10)	0.26(1)#
12	2325(7)	0.10(1)			
13	2380(3)	0.10(1)#			0.11(2)#
14	2410(3)	0.070(8)#			
15	2424(2)	7.45(36),0.05(1)#	7.4(8)	7.84(12)	
16	2514(5)	0.56(5),0.46(1)#	0.8(2)	0.7(2)	0.60(2)#
17	2638(3)	0.037(5)#			
18	2779(7)	0.086(7),0.064(1)#	0.12(2)		(0.6(2)#)[b]
19	3003(3)	0.015(1)			
20	3130(10)	0.037(5)#	0.05(1)		
21	3356(2)	20.50(13)	20.50(13)	20.50(13)	
22	3603(4)	0.060(6),0.044(1)#	0.17(2)#		0.049(8)#
23	3653(3)	0.050(3)#	0.08(2)#		0.066(6)#
24	3735(5)	0.063(6)	0.22(2)		
25	3785(7)	0.037(4)#			0.11(1)#
26	4006(3)	0.21(1)	0.25(2)	0.21(4)#	0.22(2)
27	4126(3)	0.002(1)			
28	4161(3)	0.004(1)			
29	4197(3)	0.003(1)			
30	4352(3)	0.12(1),0.035(5)#	0.15(2)		0.15(1)
31	4527(3)	0.092(4)	0.11(1)#	0.10(2)	0.11(1),<0.0062#
32	4625(7)	0.028(5)#	0.04(1)#		0.03(1)#

Peak Number	E_p(keV) This Work	BR (%) This Work	BR (%) Ref. [4]	BR (%) Ref. [5]	BR (%) Ref. [6]
33	4670(5)	0.006(1)			
34	4775(3)	0.006(1)			
35	4864(3)	0.042(5)#	0.05(1)#		0.053(6)#
36	4920(5)	0.006(1)			
37	4987(5)	0.012(1)	0.013(4)		0.021(4)
38	5054(5)	0.006(1)			
39	5138(5)	0.009(1)			
40	5305(5)	0.006(1)			
41	5350(5)	0.004(1)			
42	5445(5)	0.009(1)			
43	5510(5)	0.005(1)			
44	5560(3)	0.110(5)	0.12(1)	0.15(2)	0.16(2)
(45	5670(5)	0.013(1)	0.010(6)		0.04(2))
46	5828(3)	0.124(6)	0.09(1)		0.11(1)
47	5930(5)	0.009(1)			
48	6065(5)	0.020(2)	0.020(4)		0.023(4)
49	6350(15)	0.010(3)	0.010(4)		0.012(4)
50	6550(15)	0.005(2)			
51	6650(15)	0.002(1)			
52	6750(15)	0.002(1)			

[a] The intensity of this peak is most likely affected by the trigger threshold (see text).

[b] Observed as a broad peak centrered at 2870(5) keV in [6].

With the branching ratios to the proton-bound and proton-unbound states, the excitation energies in ^{32}Cl, the Q_{EC} and the half-life, it is possible to determine the Gamow-Teller strength B(GT) and its cumulative value in a large energy window in order to compare with shell-model calculations. We use the formula B(GT) = cte/ [(-1.2695(29))^2 f ($T_{1/2}$ / BR)] where cte = K/g_V^2 = 6144.2(16) s [28]. The results are listed in table 3.

The feeding to the ^{32}Cl ground state has been reported to be smaller than 2% [4], which corresponds to a log(ft) value larger than 5.7. The mirror decay, ^{32}Si(g.s.)$\longrightarrow$ ^{32}P(g.s.), has a log(ft) value of 8.2(1). This very large log(ft) value for a $0^+\longrightarrow 1^+$ transition is due to its ℓ-forbidden character. Assuming perfect mirror symmetry, we obtain for our case a branching ratio of $5.9(3)\times10^{-3}$ %. This value is consistent with the experimental limit and is adopted for the feeding of the ^{32}Cl ground state.

To determine the B(GT) distribution from the proton-bound states, we calculate the total $\beta\gamma$ branching ratio as 100% minus our total βp branching ratio and the β decay to the ground state. We assumed that γ decay from proton-unbound states is

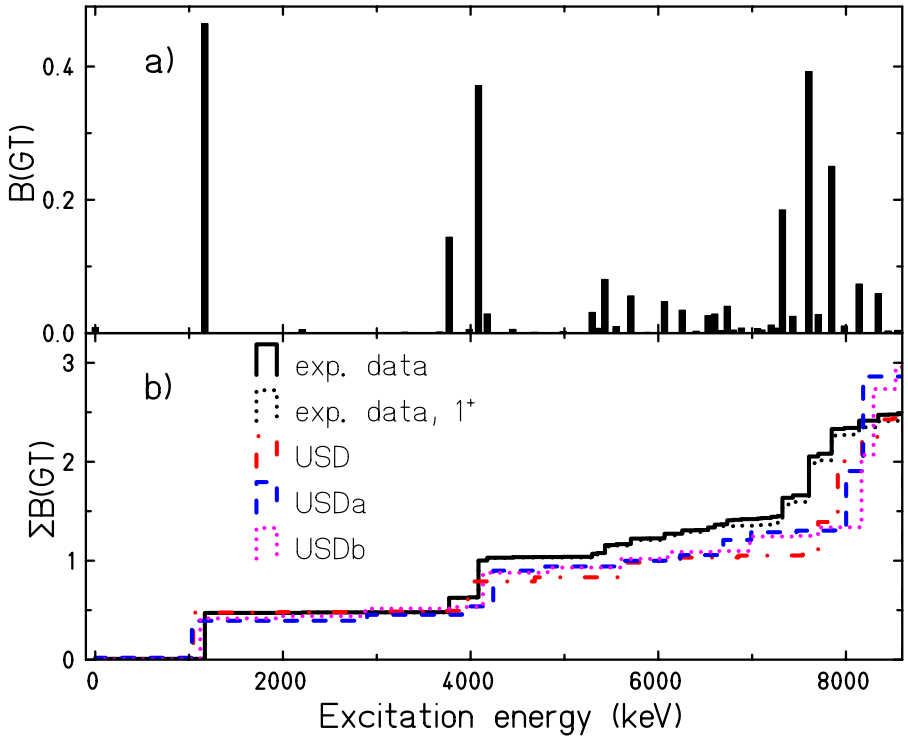

Figure 4. *a) Experimental B(GT) strength distribution for ^{32}Ar. All identifed states are shown. b) Comparison of the summed experimental B(GT) strength with the summed theoretical B(GT) strength distributions for individual transitions from shell-model calculations using the USD, USDa, and USDb effective interactions [23, 24], a curve is also shown, where we used only the states (tentatively) identified as 1^+ states. A quenching factor of 0.5 was used for the predictions.*

negligible except for the de-excitation found in [6] for the IAS with a branching ratio of 1.92(9)%. The uncertainty in β feeding to the ^{32}Cl ground state has a small effect on the final result, but rather affects the error of the $\beta\gamma$ branching ratio. With a total βp branching ratio of 35.3(2)%, we obtain 64.7(10)% for the $\beta\gamma$ decay. If the γ decay from the IAS in ^{32}Cl (1.92(9)%) is subtracted, we obtain a feeding to the 1168.5(2) keV state in ^{32}Cl of 62.8(10)%.

Comparing our total β-delayed proton branching ratio (35.3(2)%), obtained by summing all the branching ratios for proton transitions in table 2, with the value of Bhattacharya *et al.* [6] of 35.58(22)%, we obtain very good agreement.

In figure 4a), we show the experimental B(GT) distribution for all levels for all levels assigned in this work. In figure 4b), we compare the summed B(GT) distribution with the theoretical shell model predictions with different effective interactions [23, 24] using a 0.5 quenching factor for the theoretical calculations. All these calculations reproduce the main experimental characteristics mainly at low excitation energy in ^{32}Cl up to the IAS. The summed experimental B(GT) value (see figure 4b and table 4) matches best with USDb shell-model calculations [23, 24], but we observe an excess in

the experimental B(GT) sum above 4 MeV and the shape differs above 7.5 MeV. This is also the case, if we use only the states identified or tentatively identified as 1^+ states.

For a more quantitative comparison, we have calculated the quenching factor from the summed B(GT) distribution within different energy intervals. The results can be seen in table 4. The comparison with models yield quenching factors of 0.5, as expected for sd shell nuclei, for levels in ^{32}Cl up to 4 MeV. As the excitation energy increases, the quenching factors tend to differ from this average value of 0.5, but when we reach the full energy range of this study (8.6 MeV excitation energy in ^{32}Cl), the calculations agree again with the expected value.

A possible explanation for the disagreement at mid-excitation energies is that we are assigning GT strength to lower energies when it is supposed to be at higher energies. If any of the p_0 or p_1 proton transitions has a p_2 component, the B(GT) strength associated with that transition will be partially shifted to higher energies. But neither the energetics nor the penetrability favoured this possibility as the 2235.6 keV excited state in ^{31}S has spin/parity of $5/2^+$. Therefore, proton emission from excited states fed by an allowed β transition to this 2235.6 keV state will be only possible with an angular momentum ℓ=2, be it both from the IAS (0^+) or from the 1^+ states. This means that the p_2 proton decay from the IAS in this experiment has an upper branching ratio limit of 1.2×10^{-3} %, a factor of 10 lower than the measured p_1 branch. Furthermore, the main de-excitation mechanism of the level at 2235.6 keV in ^{31}S is a γ transition to the ground state [29]. We have evaluated the detection limit of our experiment based on the proton-gated γ spectrum (see figure 2c). From the peak areas in this spectrum and the γ efficiencies at 1248.4 keV and 2235.6 keV, we obtain a ratio limit of N_{p2}/N_{p1} of 0.54% which means that less than 0.03% of the decays of ^{32}Ar go through the second excited state of ^{31}S.

From the information gathered in this work, we have elaborated a decay scheme that can be seen in figure 5. Branching ratios and log(ft) values are given. Previously known J^π values are given as well. Levels fed with a log(ft) value lower than 5 are considered allowed transitions and a 1^+ spin/parity value has been assigned. Levels fed with log(ft) values between 5 and 5.9 are tentatively considered allowed transitions and the spin/parity is given as (1^+). According to the compilation of Singh *et al.* [30], less than 1% of all known forbidden transitions have a log(ft) value smaller than 5.9. For instance, the state at 4080(7) keV was tentatively assigned a spin/parity value of (1-3)$^+$ in [21]. As this level is fed by the allowed β decay of ^{32}Ar (log(ft)=4.01), we can conclude that the state has a spin/parity of 1^+. Proton emission from all these levels to the ground or to the first excited states in ^{31}S can proceed via ℓ=0 transitions and are thus not hindered by the angular momentum barrier.

Table 3. List of levels in ^{32}Cl fed by ^{32}Ar β^+ decay. We compare the excitation energies deduced for these states in the present work with previous reaction studies [21, 22] and assign spin/parity values based on log(ft) values (see text). Energies in the fourth column are always for proton energies, except those labeled by $^{\gamma}$ that are for γ-rays. Experimental B(GT) values are given for each individual transition. Excitation energies have been calculated from the proton energies in the center of mass (E_{CM}=E_p×1.032532(2)), the proton separation energy 1581.06(62) keV [6], and the energy of the γ-ray (1248.8(3) keV) in the case of transitions to the first excited state in ^{31}S. The B(GT) strength of the ground state is not included in $\sum$B(GT) as it is expected to be negligible.

E_x (this work)	E_x(^{32}Cl) [21, 26]	J^π	E_γ/E_p (keV)	BR (%)	log(ft)	B(GT)	$\sum$B(GT)
0	0	1^+	–	<2%	>5.67	<0.0082	
1168.3(12)	1168.5(2)	1^+	707.4(2)$^\gamma$	36.5(18)	3.91	0.4671	0.4671
			1078.7(2)$^\gamma$	12.0(7)			
			1168.5(5)$^\gamma$	14.2(7)			
2204(4)	2209.5(5)[a]	1^+	603(4)	0.38(1)[b]	5.88	0.0051	0.4722
2650(10)	2665(10)		1035(10)	0.034(4)	6.80	0.0006	0.4728
2925(2)	2941(5)		1302(2)	0.006(1)	7.48	0.0001	0.4729
3299(3)	3290(10)		1664(3)	0.051(2)	6.44	0.0014	0.4743
3672(7)	3692(7)		2025(7)	0.048(2)	6.35	0.0017	0.4760
3773(3)	3730(100)	1^+	909(10)	0.029(3)	4.42	0.1450	0.6210
			2123(3)	3.8(2)			
3987(6)	4002(6)	(1^+)	1130(10)	0.023(3)	5.84	0.0055	0.6265
			2325(7)	0.10(1)			
4085(2)	4080(7)	1^+	1218(3)	0.35(3)	4.01	0.3739	1.0003
			2424(2)	7.45(36)			
4177(5)		1^+	2514(5)	0.56(5)	5.12	0.0288	1.0292
4450(7)		(1^+)	2779(7)	0.086(7)	5.84	0.0055	1.0347
4682(3)			3003(3)	0.015(1)	6.51	0.0012	1.0358
4985(5)			2087(5)	0.022(5)	6.23	0.0022	1.0381
5047.5(16)	5046.3(4)[d]	0^+	2146(3)	0.23(2)	3.19		
			2838(1)$^\gamma$	0.24(3)[d]			
			3356(2)	20.50(13)[d]			
			3878(1)$^\gamma$	1.58(8)[d]			
			5046(1)$^\gamma$	0.10(2)[d]			
5299(3)		1^+	2390(4)[c]	0.17(1)	5.09	0.0313	1.0694
			3603(4)	0.060(6)			
5350(10)	5340(50)	(1^+)	2440(10)	0.05(1)	5.73	0.0071	1.0765
5434(3)	5466(6)	1^+	2514(5)	0.46(1)	4.67	0.0812	1.1577
			3735(3)	0.063(6)			
5550(2)	5578(8)	(1^+)	2638(3)	0.037(5)	5.60	0.0096	1.1673
			3841(3)	0.018(1)			

E_x (this work)	E_x(^{32}Cl) [21, 26]	J^π	E_γ/E_p (keV)	BR (%)	log(ft)	B(GT)	∑B(GT)
5715(3)		1^+	2779(7)	0.064(1)	4.83	0.0566	1.2239
			4006(3)	0.21(1)			
5841(3)	5813(7)		4126(3)	0.002(1)	6.91	0.0005	1.2244
5877(3)			4161(3)	0.004(1)	6.59	0.0010	1.2253
5915(3)	5905(7)		4197(3)	0.003(1)	6.70	0.0008	1.2261
6074(2)	6076(8)	1^+	3130(10)	0.037(5)	4.90	0.0478	1.2740
			4352(3)	0.12(1)			
6255(3)	6290(100)	1^+	4527(3)	0.092(4)	5.04	0.0346	1.3085
6403(5)			4670(5)	0.006(1)	6.15	0.0027	1.3112
6512(3)		1^+	3603(10)	0.044(1)	5.17	0.0257	1.3369
			4775(3)	0.006(1)			
6602(3)		1^+	3653(3)	0.050(3)	5.12	0.0288	1.3657
6661(5)	6680(15)		4920(5)	0.006(1)	6.01	0.0037	1.3694
6733(5)		1^+	3785(7)	0.037(4)	5.05	0.0335	1.4030
			4987(5)	0.012(1)			
6799(5)	6820(15)	(1^+)	5054(5)	0.006(1)	5.92	0.0045	1.4075
6886(5)		(1^+)	5138(5)	0.009(1)	5.70	0.0076	1.4151
7059(5)		(1^+)	5305(5)	0.006(1)	5.77	0.0065	1.4215
7105(5)		(1^+)	5350(5)	0.004(1)	5.92	0.0046	1.4262
7203(5)		(1^+)	5445(5)	0.009(1)	5.50	0.0121	1.4382
7270(5)		(1^+)	5510(5)	0.005(1)	5.71	0.0074	1.4457
7323(3)	7360(100)	1^+	4352(3)	0.035(5)	4.21	0.2347	1.6803
			5560(3)	0.110(5)			
7435(5)	7434(20)	1^+	5670(5)	0.013(1)	5.18	0.0252	1.7056
7600(3)	7580(20	1^+	4625(7)	0.028(5)	3.99	0.3914	2.0970
			5828(3)	0.124(6)			
7704(5)	7720(100)	1^+	5930(5)	0.009(1)	5.14	0.0279	2.1249
7850(3)	7831(20)	1^+	4864(3)	0.042(5)	4.18	0.2535	2.3784
			6065(5)	0.020(1)			
7983(15)		(1^+)	6200(15)	0.002(1)	5.55	0.0107	2.3891
8138(15)	8130(20)	1^+	6350(15)	0.010(1)	4.71	0.0742	2.4633
8344(15)	8300(100)	1^+	6550(15)	0.005(1)	4.81	0.0589	2.5231
8447(15)			6650(15)	0.0002(1)	6.09	0.0031	2.5262
8551(15)	8600(100)	(1^+)	6750(15)	0.0002(1)	5.97	0.0041	2.303

[a] From [11].

[b] Average from references [4, 5, 6].

[c] Average of the proton peaks in the γ-gated proton spectrum at 2380(3) and 2410(3) keV.

[d] From reference [6].

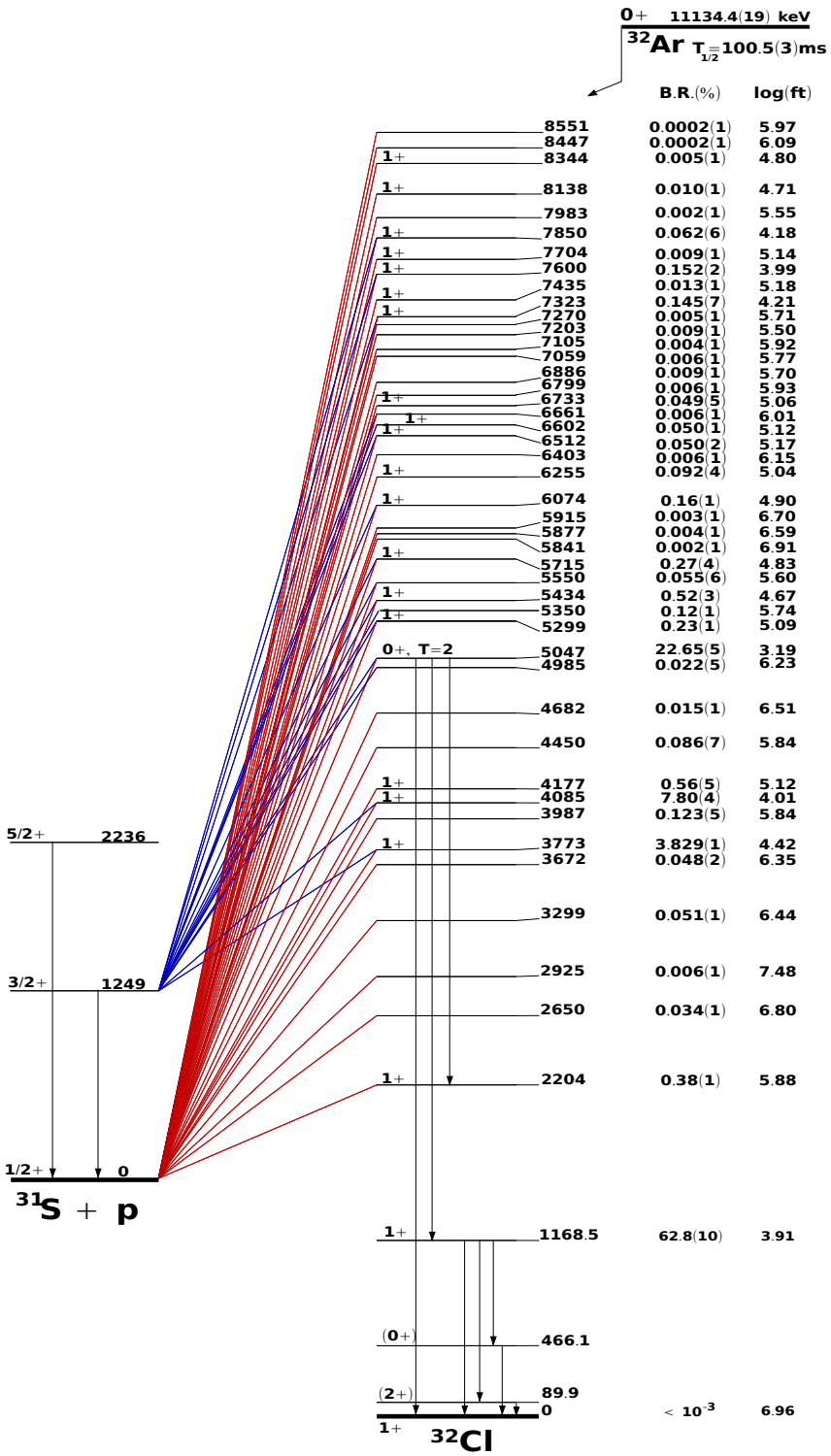

Figure 5. *Partial ^{32}Ar β^+ decay scheme. Transitions to the ^{31}S ground state and to the first excited state are shown. Branching ratios and log(ft) values for the feeding of all states are given. The IAS branching ratio is taken from reference [6]. Spin and parities are assigned from the log(ft) values (see text). The feeding to the ^{32}Cl ground state is deduced from the mirror decay.*

Table 4. Summed experimental and shell-model B(GT) distributions calculated up to the indicated limits. Quenching factors deduced from these values for each effective interaction agree with values accepted for the sd shell below 4 MeV and in the full energy range (8.6 MeV).

E limit (MeV)	Exp. ∑B(GT)	USD ∑B(GT)	USDa ∑B(GT)	USDb ∑B(GT)	q^2 USD	q^2 USDa	q^2 USDb
4	0.63(7)	1.071	1.06	1.58	0.59(6)	0.59(6)	0.40(4)
7	1.42(12)	2.56	2.45	2.10	0.55(5)	0.58(5)	0.68(6)
8	2.39(14)	2.61	2.67	4.01	0.92(5)	0.90(5)	0.60(3)
8.6	2.53(15)	5.23	5.47	4.87	0.48(3)	0.46(3)	0.52(3)

In spite of the large isospin symmetry breaking correction predicted for the ^{32}Ar $0^+ \longrightarrow 0^+$ transition, it is surprising that in none of the USD calculations a 0^+ state is predicted near the IAS. We find an 1^+ state 250 keV above the IAS and a level at 62(5) keV below the IAS. The β transition to the latter has a log(ft) value of 6.2(12). This value is a bit too low for an isospin forbidden $0^+ \longrightarrow 0^+$ transition as the known log(ft) values are according to [30] between 6.4 to 8.17 for nuclei with A $<$ 100. But it cannot be excluded due to the large uncertainty. It is argued in [31] that in the A = 32, T = 2 quintet a cubic term in the isobaric mass multiplet equation (IMME) is needed. The authors adressed the three aspects of isospin mixing using different interactions, USD [32], USDa and USDb [24]. They argued that the energy difference needed for a single T=1 state in ^{32}Cl to reproduce the coefficient of the cubic term is 73 keV for an average of the matrix elements for the three interactions. The level at 4985(5) keV identified from our γp coincidence data fulfils the energy requirement and could be responsible for the strong isospin symmetry breaking correction found recently [6]. While the log(ft) value argument is not conclusive for this level to be responsible of the mixing with the IAS, the level should however have a similar decay pattern to the one of the IAS. This means that a βp peak at around 3297(5) keV in the βp spectrum should be observed. Although a shoulder on the right hand side of the IAS proton peak is observed, our resolution does not allow to draw any firm conclusion.

6. Summary

We have performed a rather complete study of the β^+ decay of ^{32}Ar through coincident proton and γ-ray spectroscopy. Using an experimental setup with high geometric proton detection efficiency, high granularity and high γ-ray detection efficiency, we have been able to extend the knowledge about this β^+ decay and new states in ^{32}Cl have been established. We have detected new transitions to the ^{31}S first excited state and we have been able to separate proton transitions into their ground-state and first excited state components where two transitions overlap in energy.

Comparing our experimental results with shell-model calculations, we checked the validity of the shell-model approach near the proton drip-line. We compared the summed B(GT) distribution from our work to shell model calculations. These results, together with those recently published on the ^{33}Ar decay [13], settle the problem of the reduced quenching factor observed in the neutron-deficient argon isotopes. Differences between the summed experimental decay strength B(GT) with the one from shell model calculations could motivate a further experiment where low intensity proton transitions to the ^{31}S second excited state should be looked for.

We have determined from the γp spectrum a new level 62(5) keV below the IAS that could be partially responsible of the isospin symmetry breaking correction found in [6]. A proton transition from this state at 4985(5) keV to the ^{31}S ground state could not be ruled out. A new experiment with better resolution is needed to search for this proton transition.

Acknowledgements

We thank the GANIL staff and, in particular, the accelerator crew for their support during the experiment. We are indebted to B.A. Brown for providing us with the shell-model calculations and for sending us the paper of reference [31] prior to publication. We express our gratitude to the EXOGAM collaboration for providing us with the germanium detectors. R. Domínguez-Reyes acknowledges the support of the Spanish MEC under the FPI program, BES-2006-12480. This work was partly funded by the Conseil régional d'Aquitaine and the EU through the Human Capital and Mobility program. We acknowledge support from MICINN via contracts AIC10-D000584 and CICYT FPA2009-07387.

References

[1] Ichimura M, Sakai H and Wakasa T 2006 *Progress in Particle and Nuclear Physics* **56** 446
[2] Caurier E, Martinez-Pinedo G, Nowacki F, Poves A and Zuker A P 2005 *Rev. Mod. Phys.* **77** 427
[3] Hagberg E, Hansen E G, Hardy J C, Huck A, Jonson B, Mattsson S, Ravn H, Tidemand-Petersson P and Walter G 1977 *Phys. Rev. Lett.* **39** 792
[4] Björnstad T, Borge M J G, Dessagne P, von Dincklage R D, Ewan G T, Hansen P G, Huck A, Jonson B, Klotz G, Knipper A, Larsson P O, Nyman G, Ravn H L, Richard-Serre C, Riisager K, Schardt D and Walter G 1985 *Nucl. Phys.* **A443** 283
[5] Schardt D and Riisager K 1993 *Z. Phys. A* **345** 283
[6] Bhattacharya M, (Melconian D M D, Komives A, Triambak S, García A, Adelberger E G, Brown B A, Cooper M W, Glasmacher T, Guimaraes V, Mantica P F, Oros-Peusquens A M, Prisciandaro J, Steiner M, Swanson H, Tabor S L and Wiedeking M 2008 *Phys. Rev. C* **77** 065503
[7] Borge M, Hansen P, Jonson B, Mattson S, Nyman G, Richter A and Riisager K 1989 *Z. Phys.* **A332** 413
[8] Blaum K, Audi G, Beck D, Bollen G, Herfurth F, Kellerbauer A, Kluge H J, Sauvan E and Schwarz S 2003 *Phys. Rev. Lett.* **91** 260801
[9] Brown B A *private communication*

[10] Audi G, Bersillon O, Blachot J and Wapstra A H 2003 *Nucl. Phys.* **A729** 3
[11] Wrede C, Clark J A, Deibel C M, Faestermann T, Hertenberger R, Parikh A, Wirth H F, Bishop S, Chen A A, Eppinger K, García A, Krücken R, Lepyoshkina O, Rugel G and Setoodehnia K 2010 *Phys. Rev. C* **81** 055503
[12] Kankainen A, Eronen T, Gorelov D, Hakala J, Jokinen A, Kolhinen V S, Reponen M, Rissanen J, Saastamoinen A, Sonnenschein V and Äystö J 2010 *Phys. Rev.* **C 82** 052501(R)
[13] Adimi N, Reyes R D, Alcorta M, Bey A, Blank B, Borge M, de Oliveira Santos F, Dossat C, Fynbo H, Giovinazzo J, Knudsen H, Madurga M, Matea I, Perea A, Sümmerer K, Tengblad O and Thomas J 2010 *Phys. Rev. C* **81** 024311
[14] Matea I, Adimi N, Blank B, Canchel G, Giovinazzo J, Borge M J G, Domínguez-Reyes R, Tengblad O and Thomas J C 2009 *Nucl. Instrum. Meth. A* **607** 576
[15] Azaiez F 1999 *Nucl. Phys.* **A645** 1003c
[16] Bergmann U C, Fynbo H O U and Tengblad O 2003 *Nucl. Instrum. Meth.* **A515** 1106
[17] Lennard W N, Geissel H, Winterbon K B, Phillips D, Alexander T K and Forster J S 1986 *Nucl. Instrum. Meth.* **A248** 454
[18] Endt P 1998 *Nucl. Phys.* **A633** 1
[19] Pyle M C, García A, Tatar E, Cox J, Nayak B K, Triambak S, Laughman B, Komives A, Lamm L O, Rolon J E, Finnessy T, Knutson L D and Voytas P A 2002 *Phys. Rev. Lett.* **88** 122501
[20] Chen J and Singh B 2011 *Nuclear Data Sheets* **112** 1393
[21] Jeanperrin C, Rosier L H, Ramstein B and Obiajunwa E I 1989 *Nucl. Phys.* **A503** 77
[22] Vouzoukas S, Browne C P, Giessen U, Görres J, Graff S M, Herndl H, Iliadis C, Lamm L O, Meissner J, Ross J G, Scheller K, van Wormer L, Wiescher M, and Rollefson A A 1994 *Phys. Rev. C.* **50** 1185
[23] Brown B A and Wildenthal B H 1985 *At. Data Nucl. Data Tables* **34** 347
[24] Brown B A and Richter W A 2006 *Phys. Rev. C* **74** 034315
[25] Abbondanno et al U 1973 *Nuovo Cimento* **13A** 321
[26] Anderson B, Chittrakarn T, Baldwin A R, Lebo C, Madey R, Tandy P C, Watson J W, Foster C C, Brown B and Wildenthal B H 1987 *Phys. Rev. C* **36** 2195
[27] Wrede C, Clark J A, Deibel C M, Faestermann T, Hertenberger R, Parikh A, Wirth H F, Bishop S, Chen A A, Eppinger K, Freeman B M, Krücken R, Lepyoshkina O, Rugel G and Setoodehnia K 2010 *Phys. Rev. C* **82** 035805
[28] Hardy J C and Towner I S 2009 *Phys. Rev. C* **79** 055502
[29] Détraz C, Moss C and Zaidins C 1989 *Phys. Lett.* **34 B** 128
[30] Singh B, Rodriguez J, Wong S M and Tuli J 1998 *Nuclear Data Sheets* **84** 487
[31] Signoracci A and Brown B A 2011 *Phys. Rev. C* submitted
[32] Wildenthal B H 1984 *Prog. Part. Nucl. Phys.* **11** 5